Paper pa02-077
Submitted to the 28th International Conference on High Energy Physics
ICHEP'96, Warsaw, Poland, July 1996

Event Shape Variables in Deep Inelastic Scattering

H1 Collaboration

Abstract

Deep inelastic $e\,p$ scattering data are used to study the event shape variables thrust, jet broadening, C parameter and jet mass in the current hemisphere of the Breit frame over a large range of momentum transfer Q. The data are compared with results from e^+e^- experiments. A method is discussed, which allows the simultaneous determination of both the strong coupling constant $\alpha_s(Q)$ and the power or hadronisation corrections.

1 Introduction

Event shape variables have been successfully used in e^+e^- experiments in order to extract the strong coupling constant $\alpha_s(Q)$ independent of any event topology (*e.g.* a jet definition). In deep inelastic $e\,p$ scattering (DIS neutral current interaction) a similar analysis can be performed, provided the target fragmentation can be discarded. A particularly suited frame of reference to separate the current (quark) and target (proton) regions is the Breit frame, sketched in fig. 1. In the Breit system the purely space-like photon or gauge

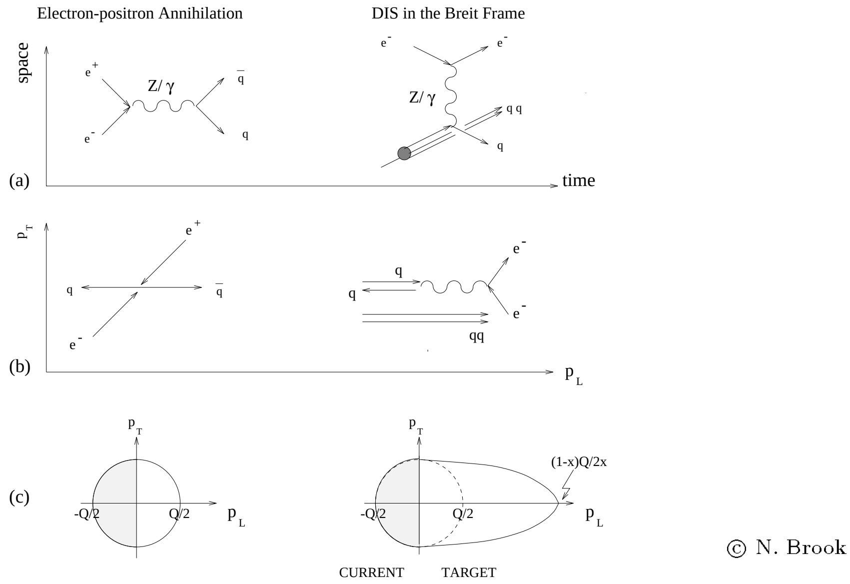

Figure 1: Definition of the Breit frame in deep inelastic $e\,p$ scattering (right), and event topology in $e^+e^- \rightarrow q\,\bar{q}$ annihilation (left)

boson Z with four-momentum $q_\gamma = \{0;\, 0, 0, -Q\}$ collides with the incoming quark with longitudinal momentum $p_{q\,z}^{in} = Q/2$. The outgoing quark is back-scattered into the current hemisphere with longitudinal momentum $p_{q\,z}^{out} = -Q/2$, while the proton fragments in the opposite target hemisphere. The phase space in the current hemisphere of the Breit frame evolves with $Q/2$. This situation can be compared with $e^+e^- \rightarrow q\,\bar{q}$ annihilation, where the phase space in one hemisphere (*e.g.* defined by the thrust axis) evolves with $Q/2 = \sqrt{s_{ee}}/2$. DIS event properties in the Breit current hemisphere should be similar and therefore comparable to those in e^+e^- collisions at a scale $Q = \sqrt{s_{ee}}$.

2 Data and Analysis Procedure

Deep inelastic $e\,p$ scattering events taken during 1994 and 1995 with the H1 detector [1] at HERA ($E_e = 27.5$ GeV, $E_p = 820$ GeV, $\sqrt{s} = 300$ GeV) are selected with the essential criteria listed in table 1. The DIS data cover a large range of momentum transfer $Q = 7 \div 100$ GeV. The scattered lepton has to be isolated within a cone of $R_e = \sqrt{\Delta\eta^2 + \Delta\phi^2} < 0.5$ around its measured direction. For the low Q event sample ($Q = 7 \div 10$ GeV, 1994

Table 1: Event selection criteria

variable	$Q = 7 \div 10$ GeV	$Q = 14 \div 100$ GeV
lepton energy	$E'_e > 10$ GeV	
lepton polar angle	$157^\circ < \theta_e < 173^\circ$	$30^\circ < \theta_e < 150^\circ$
hadron polar angles	$5.7^\circ < \theta_h < 170^\circ$	
$E - p_z$ conservation	$30 \text{ GeV} < \sum_h E_h (1 - \cos\theta_h) < 65 \text{ GeV}$	
hadronic energy in Breit current	$\sum_h E_h^c > 0.1\, Q$	
kinematic variables	$0.05 < y_e < 0.80$ and $0.05 < y_h$	

data with e^+ beam, integrated luminosity $\mathcal{L} \simeq 2.9\ pb^{-1}$) the lepton is detected in the backward electromagnetic calorimeter (BEMC). The direction is measured using the event vertex and the backward proportional chamber in front of the calorimeter. For the high Q event sample ($Q = 14 \div 100$ GeV, 1994 and 1995 data with $e^\pm$ beams, integrated luminosity $\mathcal{L} \simeq 7.7\ pb^{-1}$) the lepton is detected in the liquid Argon calorimeter. The direction is taken from an associated track measured in the central tracking system. The electromagnetic energy scales are known to 1% (BEMC, low Q leptons) and 2% (liquid Argon calorimeter, high Q leptons), respectively. For the hadrons, selected in a well measured polar angle [1] acceptance, only calorimetric information from the liquid Argon calorimeter and the instrumented iron yoke (tail catcher) is used. The hadronic energy scale is known to 5%.

The kinematic quantities Q^2, the negative squared momentum transfer, and Bjorken $x = Q^2/y\, s$ used to perform the Breit frame transformation are calculated from the electron (E'_e, θ_e) and hadron (E_h, θ_h) measurements:

$$Q^2 = 4\, E_e\, E'_e \cos^2\frac{\theta_e}{2}\,, \tag{1}$$

$$y = y_e = 1 - \frac{E'_e}{E_e}\sin^2\frac{\theta_e}{2} \qquad \text{for} \quad y_e > 0.15\,, \tag{2}$$

$$y = y_h = \frac{\sum_h E_h (1 - \cos\theta_h)}{2\, E_e} \qquad \text{for} \quad y_e < 0.15\,. \tag{3}$$

The data are corrected with a matrix method at the hadron level for detector effects (acceptance, resolution, energy scale, ...) using the LEPTO 6.1 matrix elements plus parton showers and colour dipole model Monte Carlo generators [2]. The Monte Carlo event selection is the same as for the data, but without any polar angle cuts on the hadrons. Systematic uncertainties in the data coming from the correction procedure (matrix or bin-by-bin method) and the energy scales are taken into account.

[1] Polar angles θ are defined with respect to the proton direction

3 Event Shapes in the Breit Current Hemisphere

The event shapes thrust T_c, the jet broadening B_c, the parameter C_c and the jet mass ρ_c are studied in the Breit current hemisphere. The definitions of the event shape variables are given below, where the sums extend over all hadrons h with four-momentum $p_h = \{E_h, \mathbf{p}_h\}$ fullfilling $\cos(\mathbf{p}_h \cdot \mathbf{n}) > 0$. The hemisphere axis $\mathbf{n}$ coincides with the photon direction.

- **Thrust T_c**

$$T_c = \max \frac{\sum_h |\mathbf{p}_h \cdot \mathbf{n}|}{\sum_h |\mathbf{p}_h|} \qquad \mathbf{n} \equiv \vec{T}_c \quad \text{thrust axis} \tag{4}$$

- **Jet Broadening B_c**

$$B_c = \frac{\sum_h |\mathbf{p}_h \times \mathbf{n}|}{2\sum_h |\mathbf{p}_h|} = \frac{\sum_h |\mathbf{p}_{\perp h}|}{2\sum_h |\mathbf{p}_h|} \qquad \mathbf{n} \equiv \text{hemisphere axis} \tag{5}$$

- **C_c Parameter** from the eigenvalues λ_i of the spherocity tensor $\theta^{\mu\nu}$

$$\theta^{\mu\nu} = \frac{\sum_h \mathbf{p}_h^\mu \mathbf{p}_h^\nu / |\mathbf{p}_h|}{\sum_h |\mathbf{p}_h|}$$

$$C_c = 3(\lambda_1 \lambda_2 + \lambda_2 \lambda_3 + \lambda_3 \lambda_1) \tag{6}$$

- **Jet Mass ρ_c**

$$\rho_c = \frac{M^2}{Q^2} = \frac{(\sum_h p_h)^2}{Q^2} \tag{7}$$

The results of the event shape analyses, differential distributions and mean values versus Q, are presented in figs. 2, 3, 4 and 5. The data are well described by the Monte Carlo simulation.

The differential thrust T_c distributions, shown in fig. 2a, get narrower and more peaked towards high values $T_c \to 1$ as Q or the available energy in the Breit current hemisphere increases: The energy flow becomes more collimated. This observation is supported by the mean values of $\langle 1 - T_c \rangle$ vs Q, which clearly exhibit a decrease with Q, see fig. 2b.

Similarly, the jet broadening B_c evolves from more spherical events ($B_c \to 0.5$) to jet-like events with low values of B_c as Q increases, which is also reflected in the means $\langle B_c \rangle$ vs Q, see fig. 3.

The shapes of the C_c parameter distributions, shown in fig. 4, are rather flat at low Q and get more shifted towards smaller values of C_c at large Q. Again the mean values $\langle C_c \rangle$ vs Q decrease with increasing Q.

The jet mass ρ_c spectra become narrower and shifted towards lower values with increasing Q and the mean values $\langle \rho_c \rangle$ vs Q decrease with Q, see fig. 5.

The mean thrust and jet masses of the H1 DIS $e\,p$ data in figs. 2b and 5b may be compared to e^+e^- results [3] at the scale $Q = \sqrt{s_{ee}}$. For the other variables no published e^+e^- data exist in the Q range of interest.

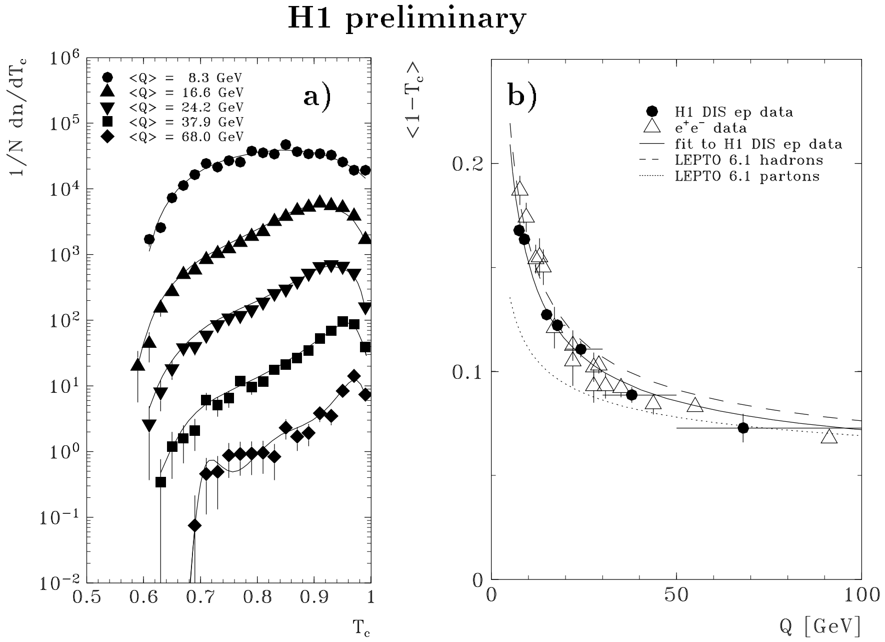

Figure 2: **a)** Thrust distributions $1/N\, dn/dT_c$ of H1 DIS $e\,p$ data (full symbols, only statistical errors shown) and Monte Carlo predictions (—). The spectra for $\langle Q \rangle = 8.3 \div 68$ GeV are multiplied by factors 10^n $(n = 0, 4)$. **b)** Mean $\langle 1 - T_c \rangle$ vs Q. H1 DIS $e\,p$ data (• and —-, errors include statistics and systematics) are compared with e^+e^- data (△) and with Monte Carlo predictions for hadrons (−−) and partons (· · ·)

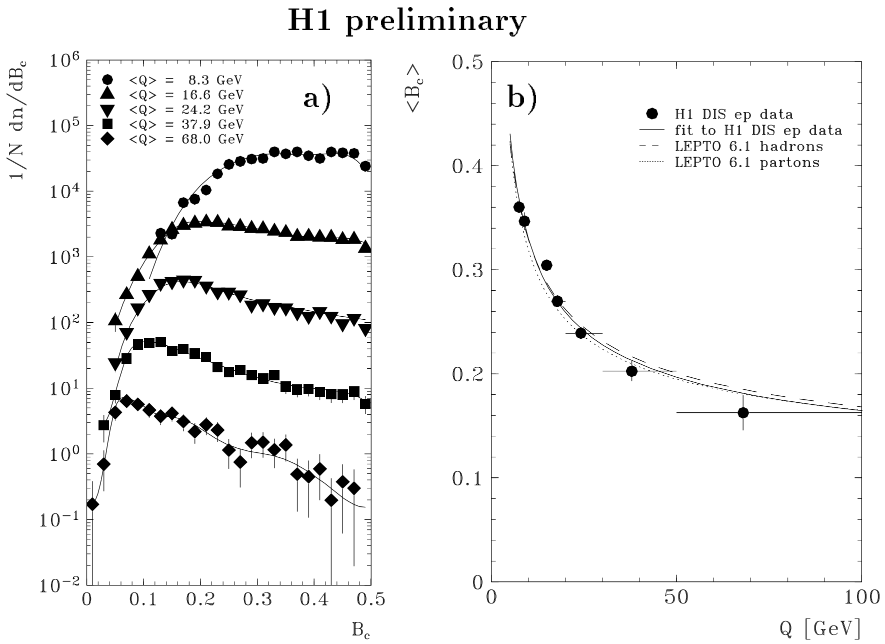

Figure 3: **a)** Jet broadening distributions $1/N\, dn/dB_c$ of H1 DIS $e\,p$ data and Monte Carlo predictions. **b)** Mean $\langle B_c \rangle$ vs Q. H1 DIS $e\,p$ data are compared with Monte Carlo predictions. Explanations and symbols as in fig. 2

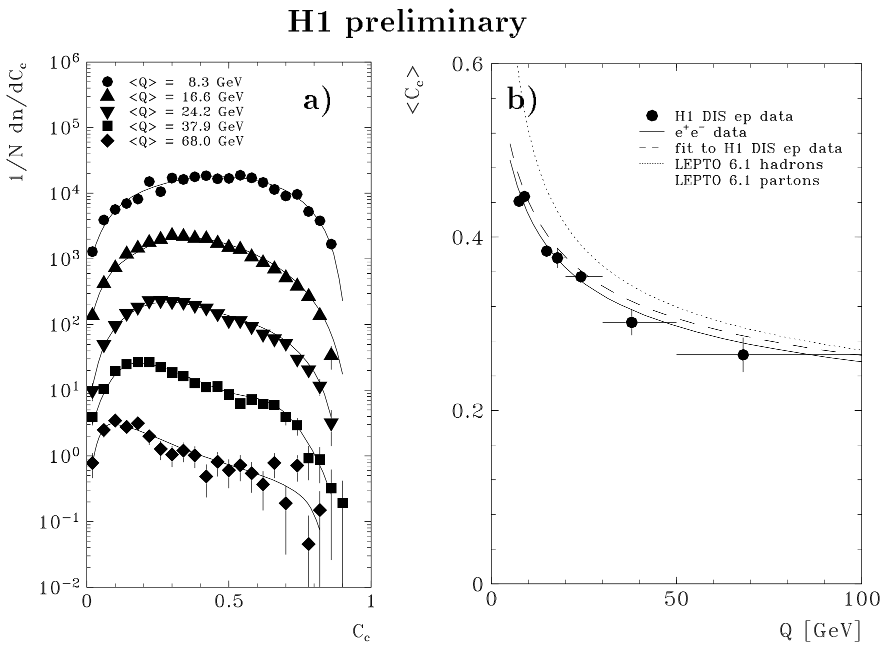

Figure 4: **a)** C parameter distributions $1/N\, dn/dC_c$ of H1 DIS $e\,p$ data and Monte Carlo predictions. **b)** Mean $\langle C_c \rangle$ vs Q. H1 DIS $e\,p$ data are compared with Monte Carlo predictions. Explanations and symbols as in fig. 2

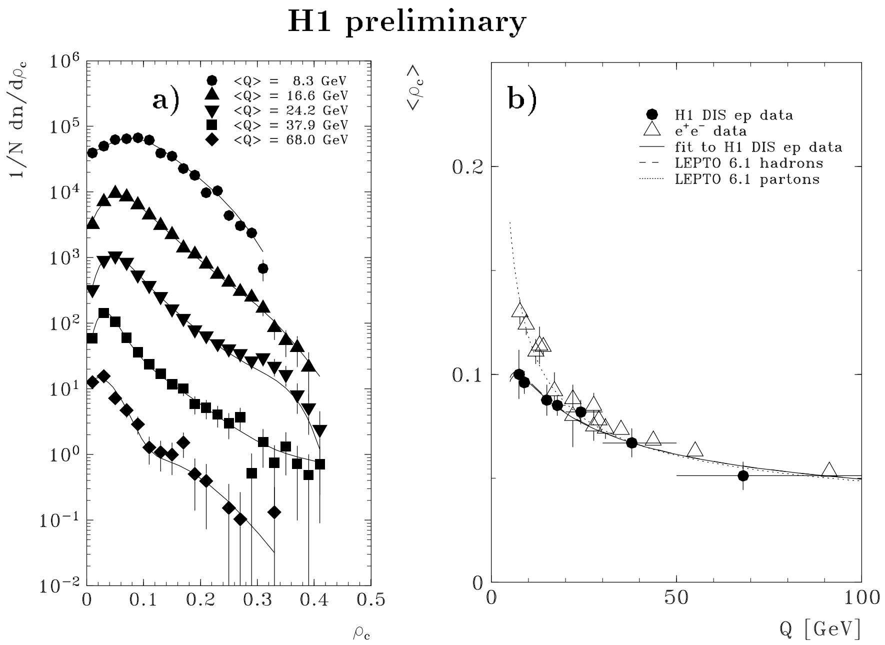

Figure 5: **a)** Jet mass distributions $1/N\, dn/d\rho_c$ of H1 DIS $e\,p$ data and Monte Carlo predictions. **b)** Mean $\langle \rho_c \rangle$ vs Q. H1 DIS $e\,p$ data are compared with e^+e^- data (heavy jet) and with Monte Carlo predictions. Explanations and symbols as in fig. 2

The distributions of $\langle 1-T\rangle$ vs Q are in gross agreement. However, the e^+e^- data, despite their relatively large errors, tend to lie systematically above the $e\,p$ data, especially at low Q. This can be qualitatively understood by the fact that in e^+e^- annihilation thrust is calculated from the whole event and not in a single hemisphere. In a two-jet event, for example, having $T_i \simeq 1$ in each hemisphere the event thrust will in general be lower, *i.e.* $T \lesssim T_i$, thus depleting the high thrust region. This behaviour is clearly borne out by comparing the $1/N\, dn/T_c$ spectra of fig. 2a with the corresponding distributions of the PLUTO and TASSO experiments [3].

The mean jet masses $\langle\rho\rangle$ vs Q in fig. 5b show a weaker Q dependence for $e\,p$ scattering than for e^+e^- collision and again the e^+e^- data are higher, in particular at low Q values. A difference is that for e^+e^- annihilation always the heavy, *i.e.* more massive jet is chosen.

There are other differences, not related to the analysis method, between deep inelastic $e\,p$ scattering and e^+e^- annihilation. The e^+e^- data contain a considerable larger fraction of bottom quarks with different fragmentation properties than the light quarks, which may be important close to threshold energies. Also the diagrams leading to the final state are different. Besides the common final state gluon radiation off quarks, DIS has contributions from initial state gluon radiation and boson gluon fusion.

Further, a 'natural' axis like the photon direction in the Breit current hemisphere of $e\,p$ scattering does not exist in e^+e^- annihilation. There the event axis is typically chosen to be the thrust axis. Such a choice can be mimicked in DIS by doing the event shape analyses analoguous to eqs. (4) – (7) but taking all hadrons in the Breit frame with $\cos(\,\mathbf{p}_h \cdot \vec{T}_c\,) > 0$, where the hemisphere axis is defined by the thrust vector $\vec{T}_c$. This selection collects more soft particles migrating between the current and target hemispheres and should affect mainly the low Q results. Fig. 6 displays for the alternative definitions, labeled with an index t, the mean values of $\langle 1-T_t\rangle$ and $\langle\rho_t\rangle$ as a function of Q. Both distributions show a stronger Q dependence compared to the standard analysis in the Breit current hemisphere and are in better agreement with the e^+e^- data at low values of Q. But there are still discrepancies at higher Q scales in the jet mass [2].

An energy or Q dependence of the event shape variables can have the following origins: (i) the logarithmic change of the strong coupling constant $\alpha_s(Q)$, and (ii) power or so-called 'hadronisation' corrections, expected to behave like $\propto Q^{-n}$. The mean value of any infrared safe event shape variable $\langle F\rangle$ in deep inelastic $e\,p$ scattering or e^+e^- annihilation can be described by [4]

$$\langle F\rangle \simeq \langle F\rangle^{\rm pert} + \langle F\rangle^{\rm pow}\ , \tag{8}$$

$$\langle F\rangle^{\rm pert} = c_1\,\alpha_s(Q) + c_2\,\alpha_s^2(Q)\ , \tag{9}$$

$$\langle F\rangle^{\rm pow} = \frac{16}{3\,\pi}\,\frac{\mu}{Q}\left[\bar{\alpha}_0(\mu) - \alpha_s(Q) - b_0\left(\ln\frac{Q}{\mu} + 1\right)\alpha_s^2(Q)\right]\ . \tag{10}$$

The perturbative part, eq. (9), represents the second order QCD prediction. The power corrections, eq. (10) with $b_0 = (33 - 2\,N_{flavour})/6\,\pi$, contain a free parameter $\bar{\alpha}_0(\mu)$ to be evaluated at some scale $\Lambda \ll \mu \ll Q$ and are expected [4] to behave like $\propto Q^{-1}$ for the

[2] A further discussion on differences between $e\,p$ and e^+e^- scattering in charged hadron multiplicities can be found in H1 Collaboration, paper pa02-072, submitted to this conference

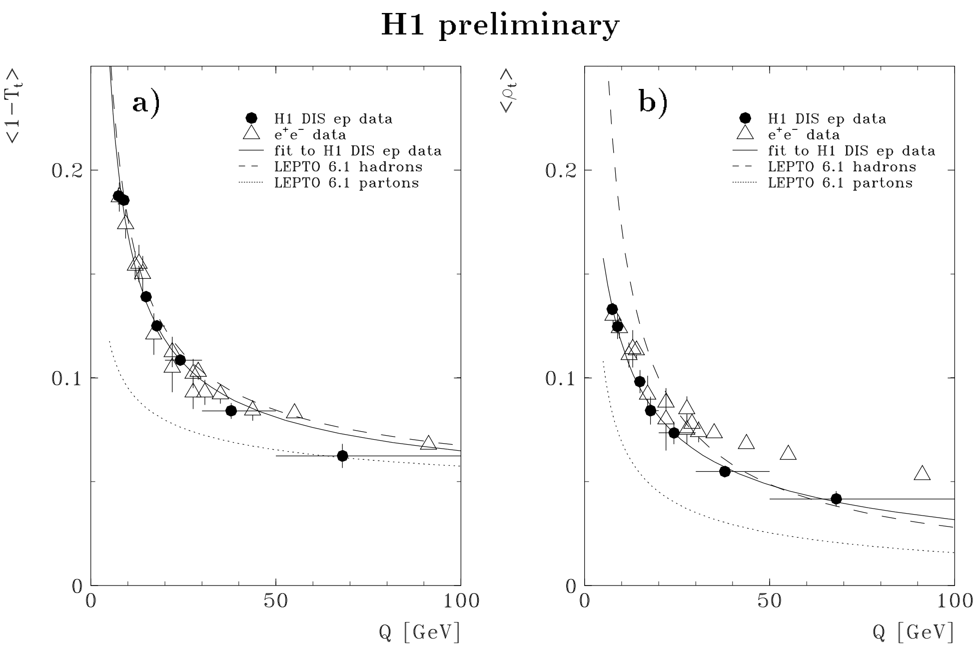

Figure 6: **a)** Mean $\langle 1-T_t\rangle$ vs Q. **b)** Mean $\langle\rho_t\rangle$ vs Q. H1 DIS $e\,p$ data ($\bullet$ and —-, errors include statistics and systematics) are compared with e^+e^- data ($\triangle$) and with Monte Carlo predictions for hadrons ($--$) and partons ($\cdots$)

event shape variables discussed in this paper. They may be due to a universal soft gluon phenomenon associated with the behaviour of the running coupling at small momentum scales. 'Universal' means that they could be expressible in terms of a few non-perturbative parameters with calculable process dependent coefficients.

The data of figs. 2b - 5b can be used to determine in a simultaneous fit $\alpha_s(Q)$ and the power corrections. For deep inelastic $e\,p$ scattering, however, perturbative next-to-leading-order calculations are not yet available. Present Monte Carlo event generators are not usable for such an analysis due to the non-unique modeling of partons in higher order (not well defined effective α_s^{eff} instead of *e.g.* $\alpha_s^{\overline{MS}}$). But one may get an idea of the amount of hadronisation contributions, becoming less important at high values of Q, by comparing the data (or Monte Carlo) with the parton curves of the LEPTO event generator in figs. 2b - 5b. In this model the hadronisation contributions are positive for $\langle 1-T_c\rangle$, negative for $\langle C_c\rangle$ and small, almost negligible for $\langle B_c\rangle$ and $\langle\rho_c\rangle$.

From a fit to the e^+e^- data one obtains for thrust $\langle 1-T\rangle_{ee}$ the values $\alpha_s(M_Z) = 0.123 \pm 0.003$ and $\bar{\alpha}_0 = 0.500 \pm 0.009$, and for the heavy jet mass $\langle\rho^H\rangle_{ee}$ the values $\alpha_s(M_Z) = 0.118 \pm 0.003$ and $\bar{\alpha}_0 = 0.417 \pm 0.005$ (only experimental errors and no scale dependence).

A similar analysis of the H1 $e\,p$ data based on the Monte Carlo parton level predictions, *i.e.* taking the coefficients c_1 and c_2 in eq. (9) from the LEPTO event generator (matrix elements plus parton showers), yields for $\langle 1-T_c\rangle$, $\langle\rho_c\rangle$ and the other shape variables experimental erros on the strong coupling constant of $\delta\alpha_s(M_Z) \simeq 0.003$. The power correction terms can be determined with errors of $\delta\bar{\alpha}_0 \simeq 0.005$ for $\langle 1-T_c\rangle$ and $\delta\bar{\alpha}_0 \simeq 0.020$

for $\langle \rho_c \rangle$. The power corrections in DIS are typically smaller than in e^+e^- scattering, but get larger and of similar size if one chooses the $\vec{T}_c$ axis to define the hemisphere, see figs. 2b, 5b and 6. This case study supports the power of event shape analyses in deep inelastic $e\,p$ scattering to determine the strong coupling constant $\alpha_s(Q)$ with an alternative method, once next-to-leading-order QCD calculations become available.

4 Conclusion

Event shape variables thrust, jet broadening, C parameter and jet mass are studied in the current hemisphere of the Breit frame in deep inelastic $e\,p$ scattering. Differential distributions and mean values are measured over a wide range of momentum transfer $Q = 7 \div 100$ GeV. The mean values of the event shapes exhibit a clear Q dependence, similar to those observed in $e^+e^- \rightarrow q\,\bar{q}$ annihilation (thrust and jet mass).

Event shape analyses in deep inelastic $e\,p$ scattering offer another possibility to determine the strong coupling constant $\alpha_s(Q)$ as well as power or hadronisation corrections with a precision comparable to e^+e^- experiments. The advantage is that a large Q range can be covered in a single experiment with high statistics. However, next-to-leading-order QCD calculations are urgently needed, either in the form of analytical formulae or Monte Carlo calculations.

Acknowledgments We are grateful to the HERA machine group whose outstanding efforts have made and continue to make this experiment possible. We thank the engineers and technicians for their work in constructing and now maintaining the H1 detector, our funding agencies for financial support, the DESY technical staff for continual assistance, and the DESY directorate for the hospitality which they extend to the non–DESY members of the collaboration.

References

[1] H1 Collaboration, I. Abt et al., *The H1 Detector at HERA*, DESY internal report H1-96-01 (1996), subm. to Nucl. Instr. and Meth.

[2] G. Ingelmann, Proceedings *Physics at HERA*, Hamburg (1991), eds. W. Buchmüller and G. Ingelmann, vol. 3, p. 1366;
L. Lönnblad, Computer Phys. Comm. 71 (1992) 15.

[3] PLUTO Collaboration, Ch. Berger et al., Z. Phys. C 12 (1982) 297;
Mark II Collaboration, A. Peterson et al., Phys. Rev. D 37 (1988) 1;
TASSO Collaboration, W. Braunschweig et al., Z. Phys. C 45 (1989) 11 and Z. Phys. C 47 (1990) 187;
AMY Collaboration, Y.K. Li et al., Phys. Rev. D 41 (1990) 2675;
DELPHI Collaboration, J. Drees et al., preprint DELPHI 96-28 PHYS 602 (1996).

[4] B. Webber, Proceedings *Workshop on Deep Inelastic Scattering and QCD*, Paris (1995), eds. J.F. Laporte and Y. Sirois, p. 115.